



Molecular and functional interactions of alpha-synuclein with Rab3a

Received for publication, March 15, 2022, and in revised form, July 1, 2022. Published, Papers in Press, July 6, 2022.
<https://doi.org/10.1016/j.jbc.2022.102239>

Guohua Lv[‡], Myung Soo Ko[‡], Tapojyoti Das[‡], and David Eliezer^{*†}

From the Department of Biochemistry, Weill Cornell Medical College, New York, New York, USA

Edited by Wolfgang Peti

Alpha-synuclein (a-Syn) is a presynaptic protein, the misfolding of which is associated with Parkinson's disease. Rab GTPases are small guanine nucleotide binding proteins that play key roles in vesicle trafficking and have been associated with a-Syn function and dysfunction. a-Syn is enriched on synaptic vesicles, where it has been reported to interact with GTP-bound Rab3a, a master regulator of synaptic vesicle trafficking. a-Syn is known to bind weakly to Rab8a in solution *via* a positively charged patch, but the physiological implications of such interactions have not been explored. Here, we investigate direct interactions between a-Syn and Rab3a in solution and on lipid membranes using NMR spectroscopy. We find that the C terminus of a-Syn interacts with Rab3a in a manner similar to its previously reported interaction with Rab8a. While weak in solution, we demonstrate that this interaction becomes stronger when the proteins are bound to a membrane surface. The Rab3a binding site for a-Syn is similar to the surface that contacts the Rab3a effector rabphilin-3A, which modulates the enzymatic activity of Rab3a. Accordingly, we show that a-Syn inhibits GTP hydrolysis by Rab3a and that inhibition is more potent on the membrane surface, suggesting that their interaction may be functionally relevant. Finally, we show that phosphorylation of a-Syn residue Ser 129, a modification associated with Parkinson's disease pathology, enhances its interactions with Rab3a and increases its ability to inhibit Rab3a GTP hydrolysis. These results represent the first observation of a functional role for synuclein-Rab interactions and for a-Syn Ser 129 phosphorylation.

Parkinson's disease (PD) is the second most common neurodegenerative disorder after Alzheimer's disease. The protein alpha-synuclein (a-Syn) is the major component of intraneuronal proteinaceous aggregates known as Lewy bodies (1) that are a diagnostic hallmark of PD. A-Syn belongs to the class of intrinsically disordered proteins and undergoes a disorder-to-helix transition upon binding to membranes and membrane mimetics (2, 3). The physiological functions of a-Syn remain to be conclusively established, but evidence suggests that a-Syn is involved in the regulation of synaptic

vesicle (SV) exocytosis (4–12) and that direct interactions with lipids and SVs are important for a-Syn function. In addition, phosphorylation at residue Ser 129, located in the acidic C-terminal tail of the protein, is the most abundant post-translational modification (PTM) of a-Syn in PD (13, 14). In Lewy bodies, 90% of a-Syn is estimated to be phosphorylated at Ser 129 (14). However, the functional role and consequences of phosphorylation at this site are largely unknown (15, 16).

Rab proteins are a subfamily of the small GTPases superfamily, which function as molecular switches that interact with downstream effector proteins in their activated, GTP-bound state and initiate a wide spectrum of cellular signaling pathways (17). Hydrolysis of GTP to GDP leads to dissociation of the effector proteins and terminates downstream events (17–21). Regulation of Rab GTPase activity provides a mechanism for controlling Rab signaling and is affected by GDP-GTP exchange factors and GTP-hydrolysis activating proteins (GAPs). GDP-GTP exchange factors and GAPs typically influence Rab activity by binding to the functionally critical switch-I and switch-II regions, which undergo conformational transitions during catalysis that are critical for GTP hydrolysis. Rab proteins play a key role in intracellular vesicular trafficking events (13, 22, 23) and have been associated with a-Syn-related neuronal function and dysfunction (8, 24–32). For example, overexpression of Rab8a, Rab1, and Rab3a attenuate a-Syn-induced cytotoxicity in cellular and animal models of PD, suggesting a functional interplay between Rab GTPases and known PD factors (8, 33). In addition, a-Syn cycling on and off SVs was reported to be influenced by the Rab3a machinery. Specifically, membrane-associated GTP-bound Rab3a stabilizes a-Syn on SVs, and the GDP dissociation inhibitor-Hsp90 complex that controls Rab3a membrane dissociation also regulates a-Syn dissociation from membranes (34).

Here, we investigate in detail the interaction of a-Syn with GTP-bound Rab3a in solution and on the surface of small unilamellar vesicles (SUVs) using NMR spectroscopy. We show that the C terminus of a-Syn binds to a positively charged patch on the surface of GTP-bound Rab3a that includes the functionally important switch-I and -II regions and that closely resembles the Rab3a binding epitope responsible for its interactions with one of its functional effectors, rabphilin-3A. This interaction is weak in solution but stronger when both proteins are localized to the membrane surface, as

[‡] These authors contributed equally to this work.

^{*} For correspondence: David Eliezer, dae2005@med.cornell.edu.

Present address for Guohua Lv: Division of Histology & Embryology, Medical College, Jinan University, Guangzhou 511486, Guangdong, China.

Functional interactions of synuclein with Rab3a

would be the case *in vivo*. Measurements of Rab3a enzymatic activity in the absence and presence of a-Syn reveal that a-Syn is an inhibitor of Rab3a GTP hydrolysis, delineating, for the first time, a potential functional role for this interaction *in vivo*. Phosphorylation of a-Syn at residue Ser 129 (pS129 a-Syn) increases its affinity for Rab3a and enhances its inhibition of Rab3a activity, suggesting a potential functional role of this disease-associated PTM.

Results

The C terminus of a-syn interacts with GTP-bound Rab3a

To characterize whether and how a-Syn binds directly to Rab3a, we used NMR spectroscopy, a versatile tool for the analysis of protein–protein or protein–ligand interactions (35). We used an N-terminally 6-His-tagged construct (a kind gift from Dr David Lambright) encompassing the GTPase domain of Rab3a (residues 15–186), because the N and C termini of the protein are important for prenylation and targeting to membranes but are not considered necessary for nucleotide binding and hydrolysis or for interactions with effectors or regulatory proteins (36–38). We introduced the Q81L mutation into our Rab3a construct because GTP hydrolysis is impaired by this mutation (39) and Rab3a was reported to interact with a-Syn preferentially in its GTP-bound state (34). Finally, to prevent concerns pertaining to cysteine oxidation or cross-linking, we also mutated the only Cys residue in Rab3a to Ala (C137A mutation). All experiments reported, except for the GTPase activity assays, were performed using this construct, which is henceforth simply referred to as Rab3a.

We monitored two-dimensional ^1H – ^{15}N correlation spectra (heteronuclear single quantum coherence, HSQC) of

^{15}N -labeled a-Syn in the presence of increasing amounts of unlabeled GTP-bound Rab3a for changes in chemical shifts and signal intensities. Slight changes in the NMR signals for C-terminal a-Syn residues ranging from L113 to A140, including small chemical shift changes and small intensity decreases (Fig. 1, left panel), became detectable upon addition of 5 (Fig. 1, red data) or 10 (Fig. 1, black data) molar equivalents of GTP-bound Rab3a. The observed changes indicate that the C terminus of a-Syn is the primary site of Rab3a interactions and are similar to those previously reported for the interaction of a-Syn with Rab8a (40). Notably, the interaction could only be observed in the absence of salt, suggesting that it is driven largely by electrostatics. Both chemical shift and intensity changes at the C terminus of a-Syn upon addition of GTP-bound Rab3a vanished in the presence of 50 mM NaCl even at molar ratio of 1:11 and 0.5:11 (Fig. S1), although slight intensity decreases were observed for the very N terminus (residues 3–9).

A-Syn interacts with a positively charged patch on GTP-bound Rab3a that includes the switch-I and switch-II regions

To explore the binding site for a-Syn on Rab3a, we produced recombinant ^{15}N -labeled and $^2\text{H}^{13}\text{C}^{15}\text{N}$ -labeled GTP-bound Rab3a and obtained sequence-specific backbone NMR resonance assignments for the GTP-bound state of the protein. In total, 165 backbone ^1H , ^{13}C , and ^{15}N NMR assignments out of 171 nonproline residues were obtained unambiguously (Fig. 2). We then titrated ^{15}N -labeled GTP-bound Rab3a with unlabeled a-Syn. However, despite extensive efforts, we were unable to observe reproducible changes in the ^1H – ^{15}N HSQC spectrum of Rab3a in the presence of a-Syn even at

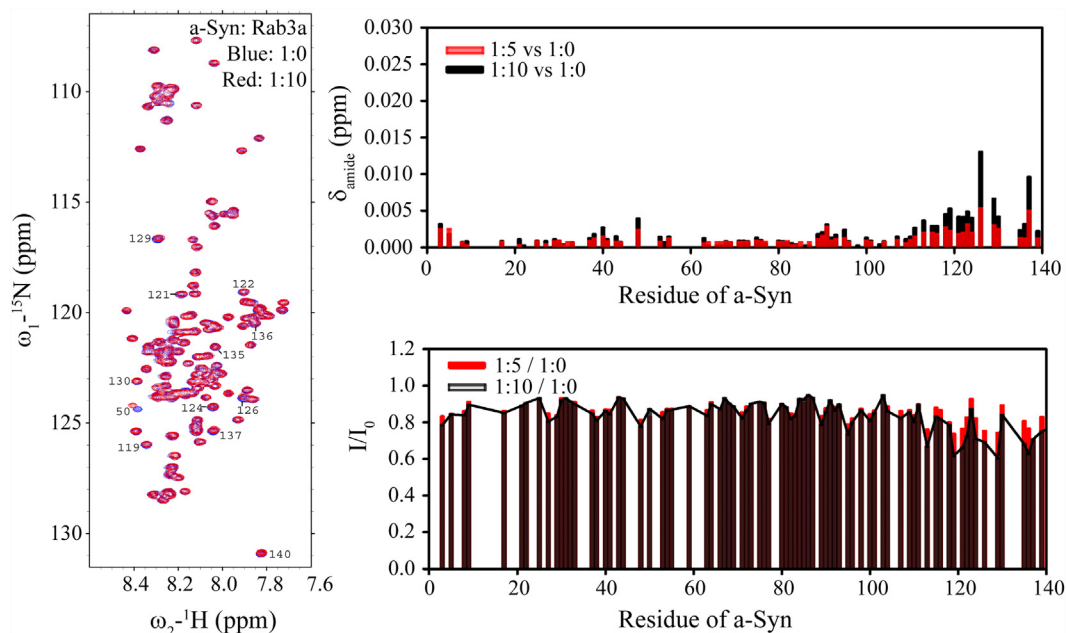


Figure 1. GTP-bound Rab3a binds to the C terminus of ^{15}N -labeled a-Syn. NMR ^1H – ^{15}N HSQC spectra of ^{15}N -labeled a-Syn in the absence (left panel, blue) or presence of 10-fold excess GTP-bound Rab3a (left panel, red) exhibit only small changes. Chemical shift changes of the amide cross peak ($\Delta\delta_{\text{amide}} = \sqrt{1/2(\Delta\delta_{\text{HN}}^2 + (\Delta\delta_{\text{N}}/5)^2)}$) upon addition of 5-fold (red) or 10-fold (black) excess Rab3a are observed at the C-terminus of the protein (right upper panel). Decreased NMR signal intensity ratios are also observed at the C terminus in the presence of 5-fold (red) or 10-fold (black) excess Rab3a (right lower panel). a-Syn, alpha-synuclein; HSQC, heteronuclear single quantum coherence.

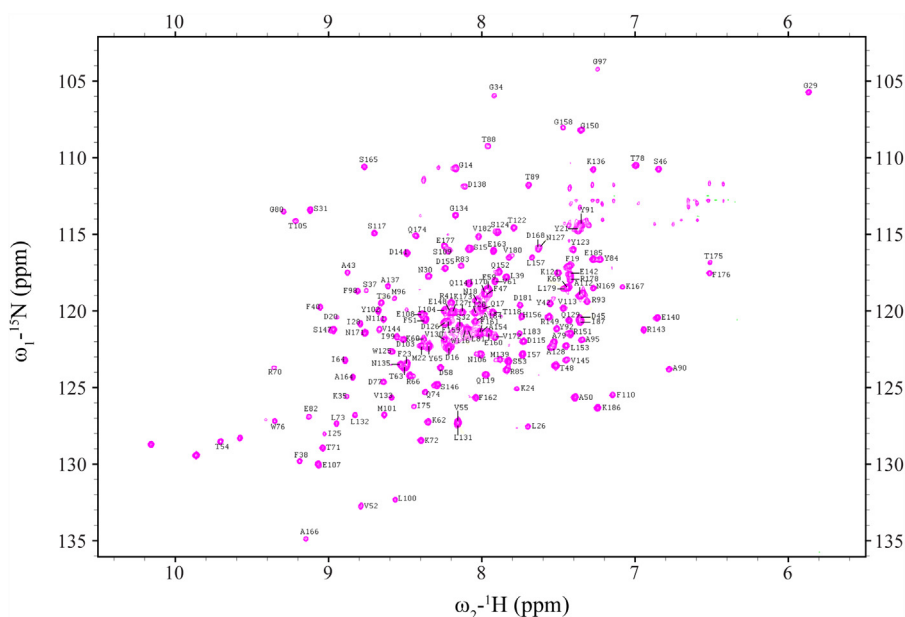


Figure 2. TROSY spectrum of $^2\text{H}^{13}\text{C}^{15}\text{N}$ -labeled GTP-bound Rab3a. Sequence-specific backbone resonance assignments are indicated.

stoichiometries as high as 20:1 α -Syn:Rab3a. As an alternative approach to identify the Rab3a binding site for α -Syn we turned to paramagnetic relaxation enhancement (PRE) measurements. PRE can establish the physical proximity of different sites within a protein or between proteins in a complex through the degree of attenuation of the NMR signals arising from the presence of a spin-labeled site. We quantified PREs as the intensity ratio of cross-peaks in the ^1H - ^{15}N HSQC spectra of a 1-oxyl-2,2,5,5-tetramethylpyrroline-3-methylmethanesulfonate (MTSL) nitroxide spin-labeled protein, in the absence and presence of ascorbic acid, which was added to the spin-labeled sample to reduce the nitroxide spin label. Residues within ~ 20 Å of the spin-labeled site are expected to exhibit attenuated intensities.

We collected PRE data for ^{15}N -labeled GTP-bound Rab3a in the presence of α -Syn spin labeled at four different sites in its C-terminal tail, as this was the α -Syn region that was observed to bind to Rab3a (Fig. 1). Spin labels were introduced by conjugating an MTSL nitroxide group to cysteine residues introduced *via* site directed mutagenesis (E110C, P120C, E130C, and A140C). Importantly, α -Syn contains no naturally occurring Cys residues. PRE effects in GTP-bound Rab3a in the presence of α -Syn spin labeled at different sites within its C-terminal tail (Fig. 3) are observed within the switch-I (residues 49–61, comprising the loop between helix-1 and strand-2 as well as part of strand-2 (38, 41)) and switch-II (residues 76–96, comprising part of strand-3, the following loop, helix-2 and the following short loop (38, 41)) regions, as well as in the vicinity of positions 20, 60 to 70, 125, 163, and 185. More specifically, PREs were observed for residues M22, V55, I57, and E163 (α -Syn_E110C); F19, M22, K24, V55, I57-D58, Y65, R70, A90, Y92, A95-M96, and W125 (α -Syn_P120C); E18, M22, I57, D58, V61, I87-T88, A90-A95, W125, E163, and E185 (α -Syn_E130C); and M22, K24, V55, I57, Y65, R70, A90, A95, E163, and E185 (α -Syn_A140C). Mapping these residues onto

the surface of the known structure of Rab3a reveals a positively charged patch (Fig. 4, left), consistent with the high negative charge content of the α -Syn C-terminal tail. Notably, the interface we identify using PREs is more extensive than that previously reported for α -Syn on the surface of Rab8a (40). In that study, binding site residues were largely restricted to helix-2 of switch-II and the G2 loop between helix-1 and strand-2, based on Rab8a chemical shift and intensity changes which, although detectable, were quite noisy. The additional binding regions, beyond helix-2 and the G2 loop that we observe here are likely also involved in α -Syn binding to Rab8a, given that Rab8a features a positively charged surface patch quite similar to that of Rab3a (Fig. 4, right), and that docking studies indicated the involvement of this entire patch in α -Syn binding to Rab8a (40).

A-Syn-Rab3a interactions are promoted by covalent linkage

Both Rab3a and α -Syn bind to SVs *in vivo*, and confinement to the small surface area of such a vesicle may promote their interactions beyond what we observed in solution. To evaluate the effect of enforced proximity on and to facilitate further characterization of this interaction, we generated a fusion construct of Rab3a (residues 15–186) Q81L and C137A with the C-terminal tail of α -Syn (residues 101–140), using a short GSGS glycine-serine linker (see methods). Note that because α -Syn is a highly disordered protein (2, 42), even a relatively short linker is not expected to restrict the ability of the highly dynamic C-terminal tail of α -Syn to reach and engage its Rab3a interaction site(s). ^1H - ^{15}N HSQC spectra of this fusion construct (Fig. 5, top) revealed an intense set of sharp peaks and a broader set of more widely dispersed peaks. The sharp signals overlay well with resonances from the C-terminal tail of α -Syn (Fig. 5, middle) and the broad, widely dispersed peaks overlay with the spectrum of Rab3a (Fig. 5, bottom). This

Functional interactions of synuclein with Rab3a

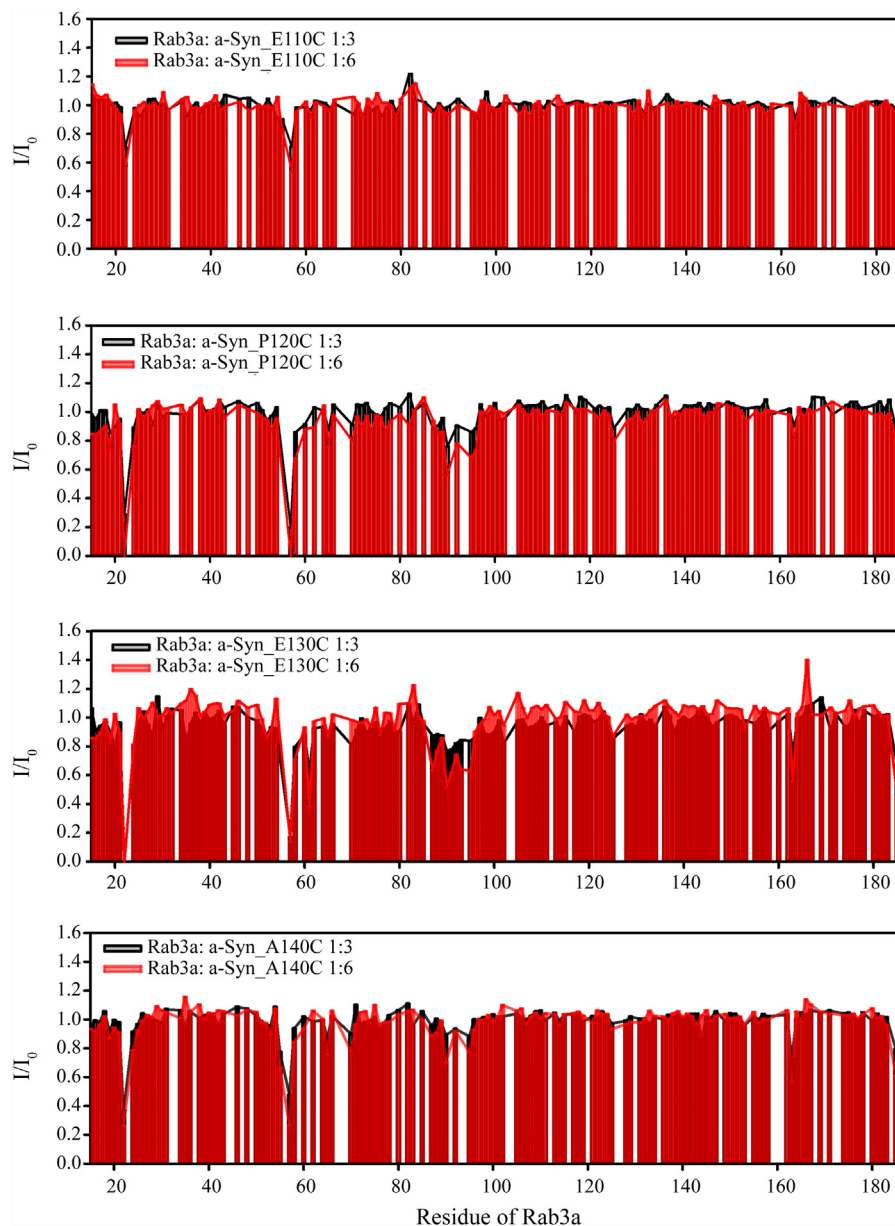


Figure 3. a-Syn interacts with the switch-I and -II region of GTP-bound Rab3a. NMR signal intensity ratios for ^{15}N -labeled GTP-bound Rab3a in the presence of ^{14}N a-Syn_E110C (top panel), a-Syn_P120C, a-Syn_E130C or a-Syn_A140C (bottom panel) spin-labeled with MTSL versus reduced by ascorbic acid at 1:3 (black) and 1:6 (red) stoichiometries. Intensity ratios below 1 indicate proximity of the spin labeled position in a-Syn to the affected region of Rab3a. a-Syn, alpha-synuclein; MTSL, 1-oxy-2,2,5,5,-tetramethylpyrroline-3-methyl-methanethiosulfonate.

indicates that the Rab3a domain of the fusion protein remains intact and that the C-terminal tail of a-Syn remains highly dynamic. Nevertheless, a detailed comparison of the Rab3a chemical shifts in the context of this fusion with those of isolated Rab3a revealed clear chemical shift changes, presumably arising from interactions between the two tethered protein domains. Resonances that exhibited the largest changes included D20, K24, I64, R66, R70, I75, R93, A95-G97, A128, and V145 (Fig. 6, top), which fall into regions that were also implicated in the PRE data above as sites of interaction between Rab3a and a-Syn. Because Rab3a chemical shift changes could not be observed upon incubation with free a-Syn, even at high stoichiometries, the observation of Rab3a

chemical shifts in the fusion construct indicates that the interaction between the two domains is stronger when they are constrained to be near each other, as expected. Small chemical shifts observed in resonances from the a-Syn C-terminal tail in the fusion construct, compared with those for a-Syn alone in solution under the same conditions (Fig. 6, bottom left), were similar to those observed with mixtures of the two individual proteins (Fig. 1).

Further evidence of a-Syn-Rab3a interactions in the context of the fusion construct was obtained from measurements of R_2 transverse relaxation rates for the sharp signals originating from the a-Syn C-terminal domain. R_2 is dependent on both overall and internal molecular mobility (43) and changes in R_2

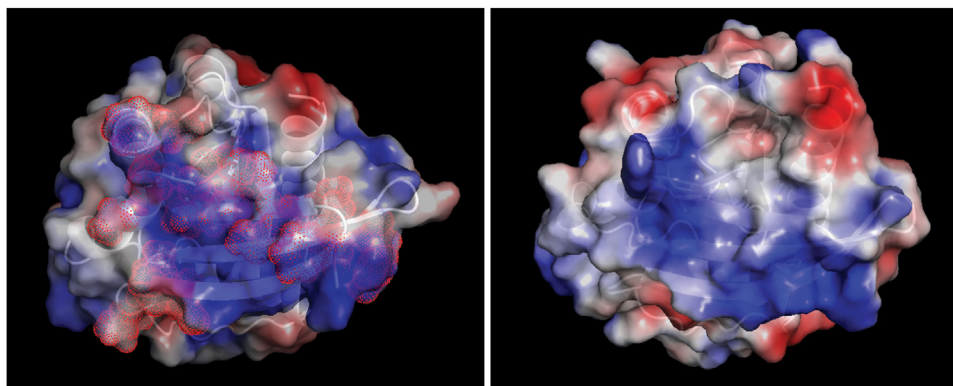


Figure 4. a-Syn binds to a positive patch on the surface of Rab3a. *Left:* The structure of Rab3a (PDB ID 3RAB residues 18–186 bound to GppNHp) colored to show surface electrostatic potential (calculated using PyMOL) with residues implicated in binding the C-terminal tail of a-Syn shown using a dot surface representation. *Right:* The structure of Rab8a (PDB ID 3QBT, residues 9–178 bound to GppNHp) colored to show surface electrostatic potential. A positive patch that was shown to bind Rab8a (40) is evident and appears similar to the a-Syn binding surface of Rab3a shown in the left panel. a-Syn, alpha-synuclein.

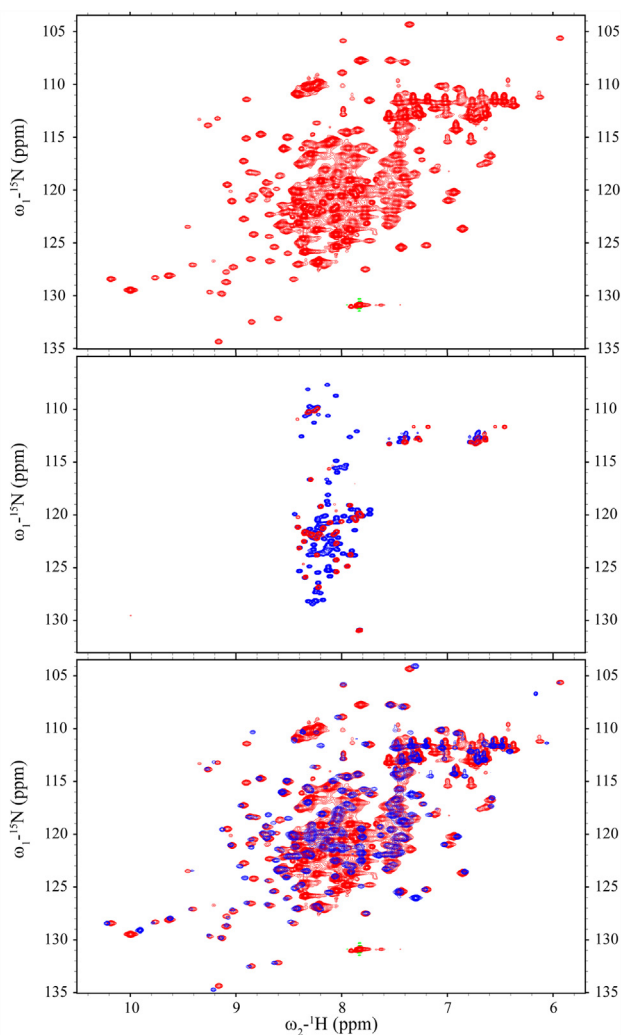


Figure 5. The C terminus of a-Syn interacts more strongly with Rab3a in the context of a fusion protein. NMR ^1H - ^{15}N HSQC spectra of ^{15}N -labeled Rab3a fused to the C-terminus of a-Syn (*top*). Intense narrow signals with limited dispersion that remain visible when the contour level cutoff is raised (*red*) correspond to resonances of free a-Syn in solution (*blue*) that originate from the C terminus of the protein (*middle*). Weaker and more widely dispersed signals (*red*) correspond to resonances from free Rab3a in solution (*blue*) (*bottom*). a-Syn, alpha-synuclein.

upon binding provide sensitive probes of molecular interactions. The C-terminal 40 residues of a-Syn exhibit higher R_2 values in the fusion protein than in isolated full length a-Syn (Fig. 6, bottom right), suggesting that they experience either a slower effective tumbling rate or broadening due to conformational exchange (or both) as a consequence of interactions with the fused Rab3a. Notably, both the chemical shifts and R_2 values of the a-Syn C-terminal domain remain characteristic of a highly disordered and dynamic polypeptide segment, indicating that the interactions between the C-terminal tail and the Rab3a domain are transient and do not lead to the formation of stable structure by a-Syn.

A-Syn-Rab3a interactions are promoted on the surface of lipid membranes

Rab3a and a-Syn are both peripheral membrane proteins, and given that covalent linkage of the proteins enhanced their interactions, we considered whether localization to membrane surfaces would have a similar effect. To localize 6-His-tagged Rab3a to membranes, we used SUVs composed of 45: 50: 5 DOPC (1,2-dioleoyl-sn-glycero-3-phosphocholine): DOPS (1,2-dioleoyl-sn-glycero-3-phospho-L-serine): DGS-NiNTA (1,2-dioleoyl-sn-glycero-3-[(N-(5-amino-1-carboxypentyl)imino)diacetic acid)succinyl]). 1D NMR experiments (not shown) confirmed binding of Rab3a to the vesicles. NMR resonances in the lipid-binding domain of a-Syn, comprising the first ~ 100 residues of the protein, exhibit decreased intensities in the presence of lipid vesicles, whereas residues in the C-terminal 40 residues of the protein are largely unaffected since this region does not interact strongly with membranes (44, 45). We compared the intensities of a-Syn ^1H - ^{15}N HSQC NMR resonances in the presence of a 400:1 ratio of lipids in the form of SUVs with and without a 5- or 10-fold excess of vesicle-bound Rab3a (Fig. 7). Resonance intensities in the C-terminal tail of a-Syn decreased by approximately 25% or 50% at the two stoichiometries (Fig. 7), compared to much smaller decreases of a few percent for the same stoichiometries in the absence of SUVs (Fig. 1). These results indicate that

Functional interactions of synuclein with Rab3a

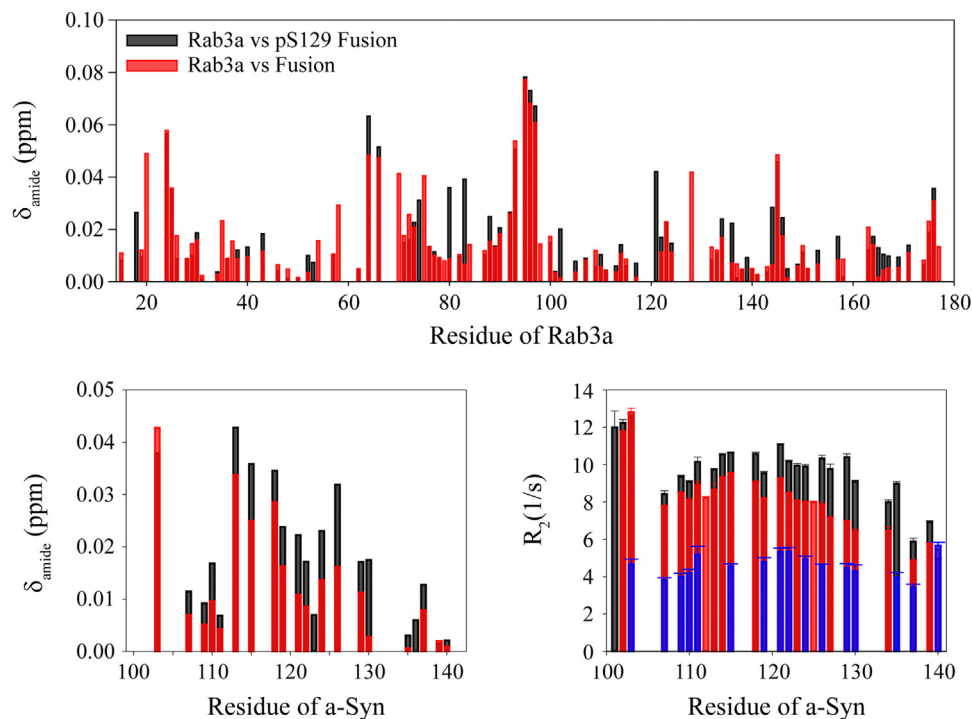


Figure 6. Rab3a interactions with a-Syn are enhanced in the context of a fusion protein. (Top) Chemical shift changes in Rab3a in the presence of the covalently attached C terminus of a-Syn indicate sites of a-Syn interaction within Rab3a. (bottom left) Chemical shift changes in the covalently attached C terminus (red) indicate sites of Rab3a interactions. Increased chemical shift changes of the amide cross peak ($\Delta\delta_{\text{amide}} = \sqrt{1/2(\Delta\delta_{\text{HN}}^2 + (\Delta\delta_{\text{N}}/5)^2)}$) for pS129 a-Syn (black) indicate that phosphorylation at a-Syn residue Ser 129 enhances Rab3a-a-Syn interactions. (bottom right) Increases in the R_2 relaxation rates for resonances in the covalently attached C terminus of a-Syn (red) compared with the same resonances in the free protein (blue) indicate interactions with Rab3a in the fusion construct. Further increases in the R_2 relaxation rates for pS129 a-Syn (black) indicate that phosphorylation at a-Syn residue Ser 129 enhance Rab3a-a-Syn interactions. a-Syn, alpha-synuclein.

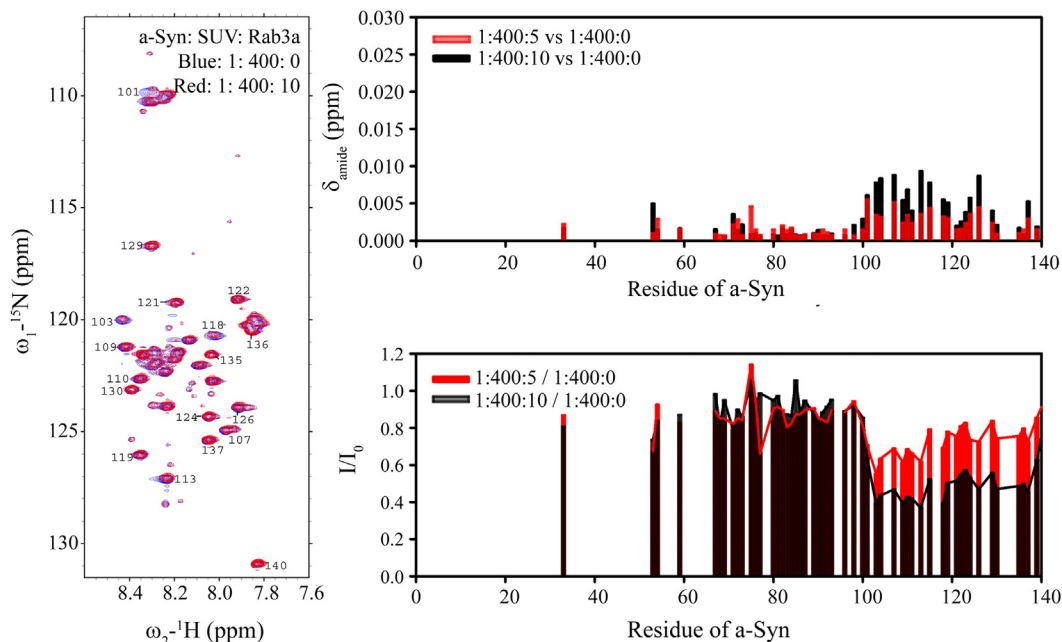


Figure 7. Rab3a interactions with a-Syn are enhanced on the surface of membranes. In the absence of Rab3a, the presence of lipid vesicles results in strong attenuation in ^1H - ^{15}N HSQC NMR spectra of signals from the N-terminal ~ 100 residues of a-Syn, but not of signals from the C-terminal tail of the protein (left panel, blue). In the presence of 5-fold (red) or 10-fold (black) excess membrane-localized Rab3a, signals from the a-Syn C-terminal tail (left panel, red) exhibit both amide chemical shift changes ($\Delta\delta_{\text{amide}} = \sqrt{1/2(\Delta\delta_{\text{HN}}^2 + (\Delta\delta_{\text{N}}/5)^2)}$, right top panel) and intensity decreases (right bottom panel). Intensity decreases are larger than those observed when the two proteins interact in the absence of membranes (compare Fig. 1). a-Syn, alpha-synuclein; HSQC, heteronuclear single quantum coherence.

colocalization of a-Syn and Rab3a to membrane surfaces significantly enhances the interaction between the proteins, consistent with the stronger interaction observed when the proteins are covalently linked and as might be expected based on reduced dimensionality and resultant higher effective concentrations of the proteins on the membrane surface.

Phosphorylation at Ser 129 of a-Syn weakly enhances interactions with Rab3a in solution, but not on membranes

Phosphorylation of a-Syn at residue Ser 129 is strongly associated with pathological a-Syn deposits in disease (16), but the physiological role of this modification is unknown. We generated pS129 a-Syn by coexpressing the protein with the polo-like kinase family member polo-like kinase 2 (PLK2) and examined its interactions with Rab3a. In solution, addition of a 10-fold excess of unlabeled Rab3a to ^{15}N -labeled pS129 a-Syn resulted in only a very slight increase in resonance attenuation in the C-terminal tail region compared to changes observed for WT a-Syn (Fig. S2) and no detectable changes in intermolecular PREs (Fig. S3). However, the fusion of Rab3a to the C-terminal tail of pS129 a-Syn resulted in a small but clear increase of chemical shift changes for both a-Syn and Rab3a, as well as in the R_2 relaxation rates of the a-Syn C-terminal residues (Fig. 6), compared to a fusion with the unmodified C-terminal tail, indicating that in the context of the fusion construct, phosphorylation of a-Syn at residue Ser 129 strengthens the interaction of a-Syn and Rab3a. Surprisingly, in the presence of SUVs, Ser 129 phosphorylation was found to result in slight decrease of membrane- and Rab3a-associated a-Syn (Fig. S4), as indicated by higher intensity ratios both in the N-terminal lipid-binding domain and in the C-terminal tail compared with unmodified a-Syn, possibly as a result of charge repulsion between the phosphate group and the negatively charged phospholipid headgroups.

GTPase activity of Rab3a is inhibited by a-Syn in solution and on membranes

The binding site for a-Syn on Rab3a mapped by PREs and chemical shift changes closely resembles the binding site for the effector domain of the Rab3a effector rabphilin-3A (41). Because rabphilin-3A alters the enzymatic activity of Rab3a (46), acting as a weak stimulator of basal GTPase activity but as an inhibitor of Rab3A GAP-stimulated activity, we examined the effect of a-Syn and pS129 a-Syn on GTP hydrolysis by Rab3a. Using a simple colorimetric assay for GTP hydrolysis (47), we found that the addition of WT or pS129 a-Syn inhibits GTP hydrolysis of Rab3a in a concentration-dependent manner, with pS129 a-Syn exhibiting a stronger effect (Fig. 8) consistent with our results indicating that Ser 129 phosphorylation enhances a-Syn binding to Rab3a. Measurements of Rab3a activity in the context of the fusion construct with the a-Syn CTD showed that covalent linkage of the proteins enhanced the ability of the a-Syn C-terminal tail to inhibit Rab3a activity. Fitting of data obtained at increasing substrate concentrations to the Michaelis-Menten equation reveals that the presence of a-Syn results in a decrease in

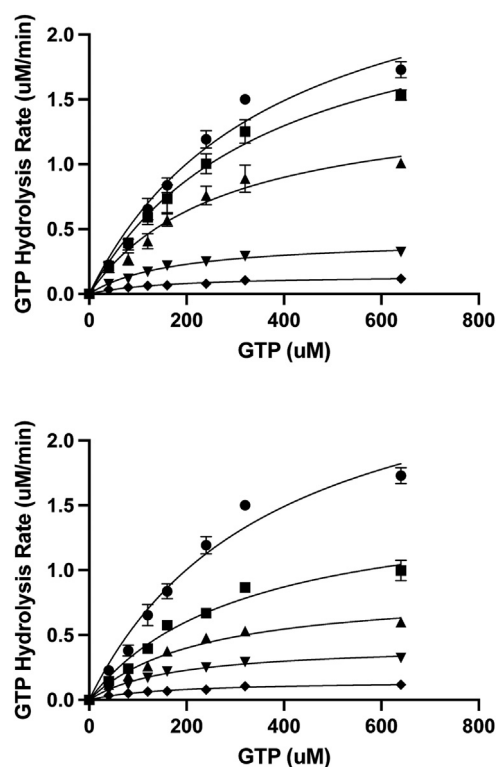


Figure 8. a-Syn inhibits the GTPase activity of Rab3a. GTP hydrolysis rates of Rab3a containing the wildtype Q residue at position 81, measured by phosphate release as a function of time at different GTP concentrations, in the absence (circles) or presence of 1:1 (upper panel) or 10:1 (lower panel) a-Syn (squares) or pS129 a-Syn (triangles) or for the fusion of the a-Syn C-terminal tail with Rab3a (inverted triangles) or for GTPase deficient Q81L Rab3a (diamonds). Measurements were performed at 37 °C at a final Rab3a concentration of 0.5 μM . Solid lines represent nonlinear least squares fits of the data to the Michaelis-Menten equation. The same data are shown for the fusion construct and the Q81L mutant in both the upper and lower panels. Error bars represent the standard deviation of three independent measurements. a-Syn, alpha-synuclein.

V_{max} , but also in a decrease in K_m (Table 1), suggesting that the protein may act as an uncompetitive inhibitor. Consistent with this possibility, the slopes of the Lineweaver-Burke plots remained roughly constant in the presence or absence of a-Syn (Fig. S5). Unexpectedly, the presence of SUVs resulted in a decreased activity of Rab3a (Fig. S6), suggesting that anchoring of this Rab3a construct to vesicles *via* its N-terminal 6-His-tag interferes with its catalytic activity. Indeed, the activity of SUV-anchored Rab3a was comparable to that observed for Rab3a in solution in the presence of 10-fold a-Syn, and addition of 1 \times or 10 \times a-Syn did not appreciably decrease the measured activity of the SUV-anchored protein further (not shown). Since Rab3a is anchored to membranes *via* prenylation of its C-terminal tail, we explored whether moving the His-tag to the C terminus of Rab3a would restore the activity of the SUV-anchored protein. Indeed, this construct resulted in an enhancement of Rab3a GTPase activity when anchored to SUVs (Fig. 9). Addition of a-Syn to this construct resulted in inhibition of enzymatic activity both in solution and in the presence of SUVs, but the effect was much greater in the presence of SUVs (Fig. 9 and Table 2), consistent with our observations of increased Rab3a-a-Syn interactions on the membrane surface

Functional interactions of synuclein with Rab3a

Table 1

Km and Vmax values for Rab3a in the absence or presence of WT or pS129 a-Syn or in the context of the Rab3a-a-Syn fusion construct

| Preparation | Km | Vmax |
|---------------------------|-------------|--------------------|
| Rab3a | 376 ± 89 μM | 2.9 ± 0.5 μM/min |
| Rab3a: WT a-Syn = 1:1 | 369 ± 73 μM | 2.5 ± 0.3 μM/min |
| Rab3a: pS129 a-Syn = 1:1 | 273 ± 71 μM | 1.5 ± 0.3 μM/min |
| Rab3a: WT a-Syn = 1:10 | 316 ± 40 μM | 1.6 ± 0.2 μM/min |
| Rab3a: pS129 a-Syn = 1:10 | 230 ± 37 μM | 0.86 ± 0.10 μM/min |
| Rab3a-a-Syn | 174 ± 46 μM | 0.43 ± 0.04 μM/min |

and with our hypothesis that this interaction is physiologically relevant. We do note that the degree of inhibition of the C-terminally tagged Rab3a construct in solution was smaller than that observed at comparable stoichiometry for the N-terminally tagged construct (Fig. 8, bottom *versus* Fig. 9). This could potentially result from the different position or the greater positive charge of the C-terminal 10-His-tag, which could perhaps screen the positively charged binding patch on the surface of Rab3a. Future studies including the intact CTD of Rab3a and with a more physiological lipid anchor will likely be required to conclusively resolve this issue.

Discussion

Despite intense interest in a-Syn in the context of its aggregation and deposition in PD and related synucleinopathies, the normal function(s) of a-Syn remain poorly understood (48–52). Beginning with its original identification as a protein enriched in synaptosome preparations from electric eels (53), a substantial body of work has implicated a-Syn as playing a functional role in the SV cycle (5, 11, 51, 54, 55). Nevertheless, mechanistic insights into how a-Syn could influence SV trafficking and release have remained sparse and have largely been confined to investigations of a-Syn interactions with SNARE proteins and its effects on SNARE-mediated vesicle fusion (6, 56–58), including fusion pore formation (59, 60). More

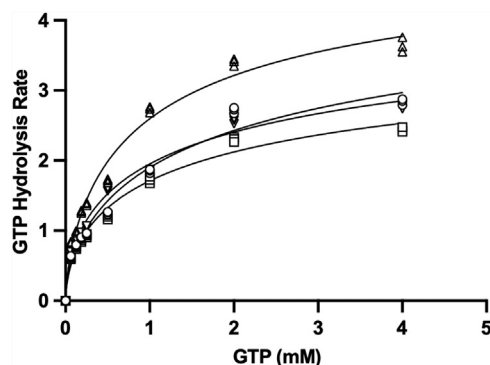


Figure 9. a-Syn inhibits the GTPase activity of C-terminally SUV-anchored Rab3a more potently than in solution. GTP hydrolysis rates of C-terminally His-tagged Rab3a measured by phosphate release as a function of time at different GTP concentrations, in solution in the absence (circles) or presence (squares) of 10:1 a-Syn or anchored to SUVs via the C-terminal His-tag in the absence (triangles) or presence (inverted triangles) of 10:1 a-Syn. Measurements were performed at 37 °C at a final Rab3a concentration of 0.5 μM. Solid lines represent nonlinear least squares fits of the data to the Michaelis–Menten equation. Error bars represent the standard deviation of three independent measurements. a-Syn, alpha-synuclein; SUV, small unilamellar vesicle.

Table 2

Km and Vmax values for C-terminally His-tagged Rab3a in solution or when anchored to SUVs in the absence or presence of 10× a-Syn

| Preparation | Km | Vmax |
|----------------------|-------------|------------------|
| Rab3a | 438 ± 63 μM | 2.8 ± 0.5 μM/min |
| Rab3a: WT a-Syn | 380 ± 59 μM | 2.5 ± 0.9 μM/min |
| Rab3a: SUV | 510 ± 52 μM | 4.0 ± 0.5 μM/min |
| Rab3a: SUV: WT a-Syn | 383 ± 36 μM | 2.9 ± 0.6 μM/min |

recent work has extended this focus to the area of SV cluster organization and the potential roles of a-Syn as a modulator of liquid–liquid phase separation processes at presynaptic nerve terminals (12, 61). Studies of pathways influenced by a-Syn in living cells have highlighted both functional and pathological interactions between a-Syn and Rab proteins (8, 27, 33, 62–65), which act as master regulators of vesicle trafficking pathways in eukaryotic cells (66). Functional interactions of a-Syn specifically with Rab3a, the primary Rab regulating SV trafficking (67), have also been reported (27, 33, 34, 68). Direct but weak interactions of a-Syn with a different neuronal Rab, Rab8a, were characterized using NMR spectroscopy (40) and demonstrated that the negatively charged C-terminal tail of a-Syn binds to a positive patch on the surface of Rab8a which is formed in part by the switch-I and switch-II regions. This interaction was shown to influence the aggregation of a-Syn, but its functional consequences were not explored.

Here, we have undertaken a study of the interactions between a-Syn and Rab3a, the master regulator of SV trafficking in neurons. We hypothesized that such interactions play a role in the normal function of a-Syn and may contribute to its regulation of the SV pathway. Using NMR, we showed that in solution, the highly negatively charged C-terminal tail of a-Syn binds weakly to a positive patch on the surface of Rab3a in a manner analogous to its interaction with Rab8a, despite the limited sequence homology between these proteins. This interaction is likely driven at least in part by electrostatics, since was disrupted in the presence of salt (Fig. S1). The weakness of the interaction and its salt dependence may both call into question its physiological relevance. However, because both a-Syn and Rab3a are expected to colocalize on the surface of SVs, at a higher effective concentration than in solution, we explored whether artificially tethering the C terminus of a-Syn to Rab3a would result in stronger interactions. NMR chemical shift perturbations and relaxation measurements confirm that binding between the two proteins is enhanced in the context of this fusion construct. We further explored whether membranes would potentiate the interactions of the proteins and found that the presence of small unilamellar lipid vesicles substantially increased the binding of a-Syn to Rab3a. This result is consistent with previous data indicating that a-Syn and Rab3a form a complex on cellular membranes but not in the cytosol (34) and support the notion that their interaction may be physiologically relevant.

To explore the functional consequences of this interaction, we noted that the binding site of a-Syn on Rab3a is highly similar to the binding site occupied by the Rab3a effector rabphilin-3A, which has been reported to alter the GTPase activity of Rab3a by stimulating basal activity but inhibiting

GAP-stimulated activity (41). We therefore assayed the effects of a-Syn on the GTP hydrolysis activity of Rab3a *in vitro*. We demonstrated that a-Syn inhibits the activity of Rab3a by decreasing V_{max} , possibly acting as an uncompetitive inhibitor, and that this effect is strongly enhanced in the context of the fusion construct between a-Syn and Rab3a. Anchoring Rab3a to SUVs using an N-terminal 6-His-tag resulted in decreased GTPase activity that was no longer sensitive to a-Syn. This suggests that this anchoring mode, in contrast with the natural anchoring *via* geranyl-geranyl groups at the end of the C-terminal hypervariable region, interferes with the activity of Rab3a. Moving the His-tag to the C terminus of Rab3a resulted in a construct that exhibits increased GTPase activity when anchored to SUVs. Inhibition of this activity by a-Syn is significantly stronger when Rab3a is anchored to SUVs than when it is free in solution (Fig. 9 and Table 2), consistent with our observations of enhanced Rab3a binding to a-Syn on the surface of SUVs. However, fully recapitulating the effects of a-Syn on the activity of membrane-anchored Rab3a will likely require assays performed with authentically prenylated Rab3a, a challenging future endeavor that is being pursued.

Phosphorylation of a-Syn at residue Ser 129 is mediated by the polo-like kinase family (69, 70) and is closely associated with pathological deposition of a-Syn in PD (16). Polo-like kinases have been implicated in the regulation of synaptic plasticity (71–73), but a specific role for PLK phosphorylation of a-Syn Ser 129 has not been reported to date, although a-Syn is also a known regulator of synaptic plasticity (74). Thus, the functional consequences of this PTM remain unknown, but its location in the C-terminal tail of the protein suggests that it could modulate intermolecular interactions involving this region. Ser 129 phosphorylation was previously reported to enhance a-Syn binding to Rab8a in solution (40), and we observe a similar enhancement of Rab3a binding here. This effect is also evident in the fusion construct between the two proteins, but surprisingly not in the presence of phospholipid vesicles, possibly as a result of decreased synuclein-membrane interactions, as was previously reported to result upon nitration of tyrosine residues in the C-terminal tail of a-Syn (75). Ser 129 phosphorylation lead to an increased inhibition of Rab3a activity by a-Syn in solution and in the context of the fusion construct, indicating a potential role for this PTM in modifying this activity of a-Syn and further implicating this activity as a physiological function of the protein *in vivo*.

Conclusions

Our results reveal that a-Syn binds to Rab3a in a manner similar to that by which it engages with Rab8a but that this interaction is potentiated when the two proteins are bound to the surface of lipid vesicles resembling SVs in size. Furthermore, we show that a-Syn binding to Rab3a results in a decreased GTP hydrolyzing activity and that this inhibition is enhanced by phosphorylation of a-Syn at residue Ser 129, a modification tightly correlated with a-Syn pathology in disease.

These observations suggest that a-Syn may function in part by binding to and regulating the activity of Rab3a on SVs, which in turn would be expected to alter their trafficking and release. This conclusion is consistent with previous reports of functional interactions between a-Syn and Rab proteins but provides new mechanistic insights into the basis of the interaction and its functional consequences.

Experimental procedures

Protein expression and purification

Recombinant WT a-Syn, a-Syn_E110C, a-Syn_P120C, a-Syn_E130C, and a-Syn_A140C were produced as previously reported (76). Briefly, for protein uniformly labeled with ^{15}N for NMR titrations or ^{14}N for PRE experiments, *Escherichia coli* BL21 (DE3) cells were transformed with a plasmid encoding a-Syn and were grown at 37 °C in minimum media containing ^{15}N ammonium chloride or ^{14}N ammonium sulfate as the sole nitrogen source. Protein expression was induced with isopropyl 1-thio- β -D-galactopyranoside at an absorbance of ~ 0.6 , for 3 to 4 h at 37 °C before harvesting by centrifugation. Purification of a-Syn proceeded as previously reported (77). The purified protein was lyophilized and stored at -80 °C.

For the expression and purification of phosphorylated a-Syn, a-Syn_E110C, a-Syn_P120C, a-Syn_E130C, and a-Syn_A140C at Ser 129, *E. coli* BL21 (DE3) cells were cotransformed with plasmids encoding a-Syn and PLK2. Quantitative phosphorylation at a-Syn residue Ser 129 was verified by 2D ^1H - ^{15}N HSQC NMR spectra for isotopically labeled protein.

A construct encompassing the GTPase domain of Rab3a (residues 15–186) preceded by an N-terminal 6-His-tag peptide in a modified pET15b vector (41) was modified by site-directed mutagenesis to incorporate the C137A and/or Q81L mutations and then used to express Rab3a in *E. coli*. BL21(DE3) cells transformed with the plasmid were grown at 37 °C in either LB media or minimum media containing ^{15}N ammonium chloride as the sole nitrogen source (for ^{15}N -labeled protein) or ^{15}N ammonium chloride and ^{13}C Glucose as the sole nitrogen and carbon source in 100% D_2O (for triply-labeled $^2\text{H}^{13}\text{C}^{15}\text{N}$ protein for backbone resonance assignments). Protein expression was induced at an absorbance of ~ 0.6 by addition of 1 mM isopropyl 1-thio- β -D-galactopyranoside, and cells were harvested after an additional 4 h at 28 °C. Cell pellets were resuspended in 50 mM Tris, pH 8.0, \pm DTT, lysed by sonication, centrifuged at 40k rpm for 1 h, and the supernatant was loaded onto a Ni-NTA-agarose column (Qiagen). After washing with 2 column volumes of 50 mM Tris, pH 8.0, 500 mM NaCl, 10 mM imidazole, \pm DTT, the fusion protein was eluted with a gradient of 20, 50, 100, and 150 mM imidazole. For NMR, fractions containing Rab3a were confirmed by sodium dodecyl sulfate polyacrylamide gel electrophoresis and were dialyzed against 50 mM Tris, pH 8.0, 10 mM MgCl_2 at least 3 times. 1 mM GTP were further added after the dialysis to obtain the GTP-bound form of Rab3a, and pH was adjusted to ~ 7.1 . For GTPase activity assay, fractions eluted with 150 mM imidazole were dialyzed against 20 mM Hepes-NaOH, pH 7.5 at least three times snap-frozen in liquid

Functional interactions of synuclein with Rab3a

nitrogen and stored at -80°C . Protein concentration was determined using a NanoDrop spectrophotometer (ThermoFisher Scientific) by UV absorbance at 280 nm with an extinction coefficient of $28,420\text{ M}^{-1}\text{ cm}^{-1}$ and MW of 21.0 kDa. To produce C-terminally His-tagged Rab3a the N-terminal 6-His-tag of the Rab3a construct described above was deleted, and a 10-His-tag was inserted after the C-terminal residue. The deletion and insertion were accomplished using the Q5 site-directed mutagenesis protocol (New England Biolabs).

A fusion construct of Rab3a Q81L and C137A residues 15 to 186 to residues 101 to 140 of a-Syn, linked by a GSGS linker, was constructed by using PCR amplification to introduce BamHI and EcoRI restriction sites before and after Rab3a and an EcoRI restriction site overlaid onto a GSGS coding sequence before a-Syn residue 101 with a SalI restriction site after a-Syn residue 140. A three-piece T4 ligase reaction of the empty BamHI/SalI digested pET15b plasmid, the BamHI/EcoRI digested Rab3a fragment, and the EcoRI/SalI digested GSGS-a-Syn101-140 fragment resulted in a new pET15b plasmid containing the desired fusion with the residual EcoRI site. Site-directed mutagenesis was used to correct the EcoRI site to the desired GSGS coding sequence, generating 6-His-tagged Rab3a Q81L 15-186 linked by a GSGS linker to a-Syn 101-140 in the pET15b vector, as confirmed by DNA sequencing. Site-directed mutagenesis was used to restore the wildtype Q residue at position 81 in the fusion construct used for activity assays. Expression and purification and storage of the fusion construct followed the protocols described above for Rab3a and S129 phosphorylation was accomplished by co-transfection with PLK2 as described above.

Preparation of SUVs

All lipid vesicle stock solutions were freshly prepared, and all samples containing lipid vesicles were kept at 4°C . Lipid vesicles (DOPC: DOPS: DGS-NiNTA 45: 50: 5) were prepared by drying mixtures of different lipids dissolved in chloroform (Avanti Polar Lipids) under nitrogen gas using a SpeedVac. The lipid mixture was resuspended using corresponding buffer (50 mM Tris, pH 8.0, 10 mM MgCl_2 , 10% D_2O , 1 mM GTP for NMR titrations, and 20 mM Hepes-KOH, pH 7.5 for GTPase), immersed in a bath sonicator for 30 min, and clarified by ultracentrifugation at 130,000g for 2 h as modified from Bussell and Eliezer (44). The supernatant was used as SUV stock solution.

NMR titrations and resonance assignment

NMR experiments were performed on 600-MHz Bruker Avance, 800-MHz Bruker Avance, or 900-MHz Bruker Avance spectrometers equipped with cryogenic probes. Two-dimensional ^1H , ^{15}N -HSQC experiments were acquired for titrations, with a typical spectral width of 25 ppm in the ^{15}N dimension and 20 ppm in the ^1H dimension. Lyophilized ^{15}N -labeled WT or pS129 a-Syn was dissolved in NMR buffer (50 mM Tris, 10 mM MgCl_2 , 10% D_2O , 1 mM GTP, pH7.1) and centrifuged (25,000 RCF) to remove large molecular weight aggregates. Titration samples were

prepared by mixing stock solutions of ^{15}N -labeled WT or pS129 a-Syn: SUV: unlabeled Rab3a to achieve the desired solute concentrations as following: 1:0:0, 1:0:5, 1:0:10, 1:400:0, 1:400:5, and 1:400:10. To make direct comparison of ^{15}N -labeled a-Syn and pS129 a-Syn, the concentrations were first assayed using UV absorbance and then further confirmed by 1D NMR. In order to monitor the effect of NaCl on a-Syn-Rab3a interaction, samples of ^{15}N -labeled WT a-Syn: unlabeled Rab3a 1:0, 1:11, and 0.5:11 were prepared for ^1H , ^{15}N -HSQC titration, using a modified NMR buffer of 50 mM Tris, 50 mM NaCl, 10 mM MgCl_2 , 10% D_2O , 1 mM GTP, 0.05% NaN_3 , pH7.1. All spectra were measured at 10°C . Protein concentrations were typically $\sim 50\ \mu\text{M}$ for ^{15}N -labeled a-Syn or pS129 a-Syn.

Two-dimensional TROSY spectra and three-dimensional HNCA, HNCOC, HNCACO, HNCACB, HNCOCACB experiments of ^2H , ^{13}C , ^{15}N -labeled GTP-bound Rab3a were acquired on 600-, 800-, or 900-MHz Bruker Avance spectrometers equipped with cryogenic probes, with a typical spectral width of 25 ppm in the ^{15}N dimension and 20 ppm in the ^1H dimension. Purified ^2H , ^{13}C , ^{15}N -labeled GTP-bound Rab3a was dissolved in NMR buffer (50 mM Tris, 150 mM NaCl, 2 mM DTT, 10 mM MgCl_2 , 1 mM GTP, 0.05% NaN_3 , 10% D_2O , pH7.1) at a concentration of $\sim 260\ \mu\text{M}$, and all spectra were measured at 10°C . Spectra were processed with NMRPipe (78) and analyzed with SPARKY (79). Resonance assignments of Rab3a $^{13}\text{C}\alpha$, $^{13}\text{C}\beta$, ^{15}N , and ^1HN nuclei were obtained manually using the triple resonance data.

Paramagnetic relaxation enhancement

WT or pS129 a-Syn E110C, P120C, E130C, and A140C mutants were used for PRE measurements (WT a-Syn contains no Cys residues). The ^{14}N -labeled proteins were spin labeled with MTSL (Toronto Research Chemicals) as described (80). Briefly, WT or pS129 a-Syn single-cys mutants in 50 mM Tris, 10 mM MgCl_2 , 10% D_2O , 1 mM GTP, pH 7.1 were incubated with ca. 20-fold molar excess MTSL (prepared in 100% DMSO) for 1 h at 37°C (900 rpm). To remove free MTSL, the mixture was then dialyzed overnight against $\sim 55\ \text{mM}$ Tris, pH 8.0, 11 mM MgCl_2 , 10% D_2O and 1 mM GTP were further added after the dialysis, and pH was adjusted to ~ 7.1 . PRE was measured by collecting ^1H - ^{15}N HSQC spectra using $\sim 150\ \mu\text{M}$ ^{15}N -labeled Rab3a: ^{14}N spin labeled WT or pS129 a-Syn variants (1:3 and 1:6) at 10°C . For control diamagnetic samples, ascorbic acid (~ 15 -fold molar excess in relation to the protein) was added to the MTSL spin-labeled sample to reduce the nitroxide spin label. The intensities of cross-peaks in the ^1H - ^{15}N HSQC spectra of both the spin-labeled and reduced samples were measured, and their ratio was calculated.

R_2 relaxation

R_2 relaxation rates were measured through a series of 11 ^1H - ^{15}N HSQC-based T_2 experiments with relaxation time delays of 0, 16, 32, 48, 64, 80, 96, 112, 128, 32, and 32 ms. The intensity decay of each cross-peak was fit to a single

exponential decay function using Sparky. All ^1H - ^{15}N HSQC spectra and R_2 relaxation experiments were acquired at 10 °C, using the same NMR buffer (50 mM Tris, 10 mM MgCl_2 , 10% D_2O , 1 mM GTP, pH 7.1) at protein concentration of ca. 360 μM . Equal protein concentrations in different samples were confirmed using 1D ^1H NMR. NMR relaxation data were processed with TOPSPIN3.2 (Bruker) and analyzed with SPARKY (79).

Rab3a GTPase activity measurements

GTP hydrolysis of a Rab3a construct containing the wild-type Q residue at position 81, as well as the C137A mutation, was measured using a colorimetric assay to detect released phosphate as previously reported (47). GTP (Roche Diagnostics GmbH) was dissolved in 20 mM Hepes-NaOH, pH 7.5 and then diluted at different concentrations in GTPase assay buffer containing 20 mM Hepes-NaOH, pH 7.5, 2 mM MgCl_2 , and 1 mM DTT. Proteins and SUVs were prepared as described above in 20 mM Hepes-NaOH, pH 7.5. GTP hydrolysis in the absence and presence of 200 μM SUV lipids and of 0.5 μM or 5 μM of WT or pS129 a-Syn was initiated by adding protein mixtures to GTP solutions in assay buffer at a final Rab3a concentration of 0.5 μM and incubating at 37 °C. At each time point, 20 μl of the reaction mixture (400 μl initial volume) was transferred to a 96-well flat bottom plate containing 5 μl of 0.5 M EDTA, pH 8.0 to stop the reaction. 150 μl of Malachite Green stock solution (1 mM Malachite Green, 10 mM ammonium molybdate in 1N HCl, filtered through a 0.2 μm Millipore membrane and covered with foil to avoid light exposure) was added to each reaction, and absorbance at 650 nm was measured using a SpectraMax M5 plate reader (Global Headquarters, LLC). All measurements were performed in triplicate. A standard curve using 10 to 100 μM Pi was measured in parallel for each experiment. Absorbance of buffer only \pm GTP was measured as a subtraction blank. Reaction rates were obtained as linear fits to early time points, and the Michaelis constant (K_m) and the maximal reaction velocity (V_{max}) for Rab3a GTPase hydrolysis were obtained from nonlinear least squares fits of the reaction rates as a function of GTP concentration to the Michaelis Menten equation using Prism 9 software (GraphPad). Controls using the Q81L mutant, which is deficient in GTP hydrolysis, were performed in the same manner. The activity of the fusion construct of Rab3a with residues 101 to 140 of a-Syn, containing C137A and the wildtype Q residue at position 81, was measured in the same manner.

Data availability

NMR chemical shift assignments for GTP-bound Rab3a have been deposited in the BMRB database (BMRB accession number 51380). All other data are available upon request to David Eliezer (dae2005@med.conell.edu).

Supporting information—This article contains supporting information.

Author contributions—D. E., G. L., M. S. K., and T. D. conceptualization; G. L. and M. S. K. data acquisition; G. L. and M. S. K. formal analysis; T. D. investigation; D. E., G. L., and M.S.K. writing-original draft.

Funding and additional information—Funding was provided by the National Institutes of Health grants R37AG019391 and R35GM136686 to D. E. The content is solely the responsibility of the authors and does not necessarily represent the official views of the National Institutes of Health.

Conflicts of interest—The authors declare that they have no conflicts of interest with the contents of this article.

Abbreviations—The abbreviations used are: a-Syn, alpha-synuclein; GAP, GTP-hydrolysis activating protein; HSQC, heteronuclear single quantum coherence; MTSL, 1-oxyl-2,2,5,5-tetramethylpyrroline-3-methyl-methanethiosulfonate; PD, Parkinson's disease; PTM, posttranslational modification; PRE, paramagnetic relaxation enhancement; SUV, small unilamellar vesicle; SV, synaptic vesicle.

References

- Spillantini, M. G., Crowther, R. A., Jakes, R., Hasegawa, M., and Goedert, M. (1998) alpha-Synuclein in filamentous inclusions of Lewy bodies from Parkinson's disease and dementia with lewy bodies. *Proc. Natl. Acad. Sci. U. S. A.* **95**, 6469–6473
- Eliezer, D., Kutluay, E., Bussell, R., Jr., and Browne, G. (2001) Conformational properties of alpha-synuclein in its free and lipid-associated states. *J. Mol. Biol.* **307**, 1061–1073
- Davidson, W. S., Jonas, A., Clayton, D. F., and George, J. M. (1998) Stabilization of alpha-synuclein secondary structure upon binding to synthetic membranes. *J. Biol. Chem.* **273**, 9443–9449
- Abeliovich, A., Schmitz, Y., Farinas, I., Choi-Lundberg, D., Ho, W. H., Castillo, P. E., et al. (2000) Mice lacking alpha-synuclein display functional deficits in the nigrostriatal dopamine system. *Neuron* **25**, 239–252
- Cabin, D. E., Shimazu, K., Murphy, D., Cole, N. B., Gottschalk, W., McIlwain, K. L., et al. (2002) Synaptic vesicle depletion correlates with attenuated synaptic responses to prolonged repetitive stimulation in mice lacking alpha-synuclein. *J. Neurosci.* **22**, 8797–8807
- Chandra, S., Gallardo, G., Fernandez-Chacon, R., Schluter, O. M., and Sudhof, T. C. (2005) Alpha-synuclein cooperates with CSPA in preventing neurodegeneration. *Cell* **123**, 383–396
- Chandra, S., Fornai, F., Kwon, H. B., Yazdani, U., Atasoy, D., Liu, X., et al. (2004) Double-knockout mice for alpha- and beta-synucleins: effect on synaptic functions. *Proc. Natl. Acad. Sci. U. S. A.* **101**, 14966–14971
- Cooper, A. A., Gitler, A. D., Cashikar, A., Haynes, C. M., Hill, K. J., Bhullar, B., et al. (2006) Alpha-synuclein blocks ER-Golgi traffic and Rab1 rescues neuron loss in Parkinson's models. *Science* **313**, 324–328
- Liu, S., Ninan, I., Antonova, I., Battaglia, F., Trinchese, F., Narasanna, A., et al. (2004) alpha-Synuclein produces a long-lasting increase in neurotransmitter release. *EMBO J.* **23**, 4506–4516
- Murphy, D. D., Rueter, S. M., Trojanowski, J. Q., and Lee, V. M. (2000) Synucleins are developmentally expressed, and alpha-synuclein regulates the size of the presynaptic vesicular pool in primary hippocampal neurons. *J. Neurosci.* **20**, 3214–3220
- Nemani, V. M., Lu, W., Berge, V., Nakamura, K., Onoa, B., Lee, M. K., et al. (2010) Increased expression of alpha-synuclein reduces neurotransmitter release by inhibiting synaptic vesicle recluster after endocytosis. *Neuron* **65**, 66–79
- Ramezani, M., Wilkes, M. M., Das, T., Holowka, D., Eliezer, D., and Baird, B. (2019) Regulation of exocytosis and mitochondrial relocation by Alpha-synuclein in a mammalian cell model. *NPJ Parkinsons Dis.* **5**, 12
- Anderson, J. P., Walker, D. E., Goldstein, J. M., de Laat, R., Banducci, K., Caccavello, R. J., et al. (2006) Phosphorylation of Ser-129 is the dominant

Functional interactions of synuclein with Rab3a

- pathological modification of alpha-synuclein in familial and sporadic Lewy body disease. *J. Biol. Chem.* **281**, 29739–29752
14. Fujiwara, H., Hasegawa, M., Dohmae, N., Kawashima, A., Masliah, E., Goldberg, M. S., *et al.* (2002) alpha-Synuclein is phosphorylated in synucleinopathy lesions. *Nat. Cell Biol.* **4**, 160–164
 15. Oueslati, A., Schneider, B. L., Aebischer, P., and Lashuel, H. A. (2013) Polo-like kinase 2 regulates selective autophagic alpha-synuclein clearance and suppresses its toxicity *in vivo*. *Proc. Natl. Acad. Sci. U. S. A.* **110**, E3945–E3954
 16. Sato, H., Kato, T., and Arawaka, S. (2013) The role of Ser129 phosphorylation of alpha-synuclein in neurodegeneration of Parkinson's disease: a review of *in vivo* models. *Rev. Neurosci.* **24**, 115–123
 17. Yin, G., Lv, G., Zhang, J., Jiang, H., Lai, T., Yang, Y., *et al.* (2022) Early-stage structure-based drug discovery for small GTPases by NMR spectroscopy. *Pharmacol. Ther.* **236**, 108110
 18. Bos, J. L., Rehmann, H., and Wittinghofer, A. (2007) GEFs and GAPs: critical elements in the control of small G proteins. *Cell* **129**, 865–877
 19. Cherfils, J., and Zeghouf, M. (2013) Regulation of small GTPases by GEFs, GAPs, and GDIs. *Physiol. Rev.* **93**, 269–309
 20. Dransart, E., Olofsson B Fau - Cherfils, J., and Cherfils, J. (2005) RhoGDIs revisited: novel roles in Rho regulation. *Traffic* **6**, 957–966
 21. Seabra, M. C., and Wasmeier, C. (2004) Controlling the location and activation of Rab GTPases. *Curr. Opin. Cell Biol.* **16**, 451–457
 22. Rivero-Ríos, P., Gómez-Suaga, P., Fernández, B., Madero-Pérez, J., Schwab, Andrew J., Ebert, Allison D., *et al.* (2015) Alterations in late endocytic trafficking related to the pathobiology of LRRK2-linked Parkinson's disease. *Biochem. Soc. Trans.* **43**, 390–395
 23. Stenmark, H. (2009) Rab GTPases as coordinators of vesicle traffic. *Nat. Rev. Mol. Cell Biol.* **10**, 513–525
 24. Wilson, G. R., Sim, J. C., McLean, C., Giannandrea, M., Galea, C. A., Riseley, J. R., *et al.* (2014) Mutations in RAB39B cause X-linked intellectual disability and early-onset Parkinson disease with alpha-synuclein pathology. *Am. J. Hum. Genet.* **95**, 729–735
 25. Mata, I. F., Jang, Y., Kim, C. H., Hanna, D. S., Dorschner, M. O., Samii, A., *et al.* (2015) The RAB39B p.G192R mutation causes X-linked dominant Parkinson's disease. *Mol. Neurodegener.* **10**, 50
 26. Chung, C. Y., Koprach, J. B., Hallett, P. J., and Isacson, O. (2009) Functional enhancement and protection of dopaminergic terminals by RAB3B overexpression. *Proc. Natl. Acad. Sci. U. S. A.* **106**, 22474–22479
 27. Dalfo, E., Barrachina, M., Rosa, J. L., Ambrosio, S., and Ferrer, I. (2004) Abnormal alpha-synuclein interactions with rab3a and rabphilin in diffuse Lewy body disease. *Neurobiol. Dis.* **16**, 92–97
 28. Dalfo, E., Gomez-Isla, T., Rosa, J. L., Nieto Bodelon, M., Cuadrado Tejedor, M., Barrachina, M., *et al.* (2004) Abnormal alpha-synuclein interactions with Rab proteins in alpha-synuclein A30P transgenic mice. *J. Neuropathol. Exp. Neurol.* **63**, 302–313
 29. Kuwahara, T., Koyama, A., Koyama, S., Yoshina, S., Ren, C. H., Kato, T., *et al.* (2008) A systematic RNAi screen reveals involvement of endocytic pathway in neuronal dysfunction in alpha-synuclein transgenic *C. elegans*. *Hum. Mol. Genet.* **17**, 2997–3009
 30. Liu, J., Zhang, J. P., Shi, M., Quinn, T., Bradner, J., Beyer, R., *et al.* (2009) Rab11a and HSP90 regulate recycling of extracellular alpha-synuclein. *J. Neurosci.* **29**, 1480–1485
 31. Sancenon, V., Lee, S. A., Patrick, C., Griffith, J., Paulino, A., Outeiro, T. F., *et al.* (2012) Suppression of alpha-synuclein toxicity and vesicle trafficking defects by phosphorylation at S129 in yeast depends on genetic context. *Hum. Mol. Genet.* **21**, 2432–2449
 32. Soper, J. H., Roy, S., Stieber, A., Lee, E., Wilson, R. B., Trojanowski, J. Q., *et al.* (2008) Alpha-synuclein-induced aggregation of cytoplasmic vesicles in *Saccharomyces cerevisiae*. *Mol. Biol. Cell* **19**, 1093–1103
 33. Gitler, A. D., Bevis, B. J., Shorter, J., Strathearn, K. E., Hamamichi, S., Su, L. J., *et al.* (2008) The Parkinson's disease protein alpha-synuclein disrupts cellular Rab homeostasis. *Proc. Natl. Acad. Sci. U. S. A.* **105**, 145–150
 34. Chen, R. H., Wislet-Gendebien, S., Samuel, F., Visanji, N. P., Zhang, G., Marsilio, D., *et al.* (2013) alpha-Synuclein membrane association is regulated by the Rab3a recycling machinery and presynaptic activity. *J. Biol. Chem.* **288**, 7438–7449
 35. Craik, D. J., and Wilce, J. A. (1997) Studies of protein-ligand interactions by NMR. *Methods Mol. Biol.* **60**, 195–232
 36. Chavrier, P., Gorvel, J. P., Stelzer, E., Simons, K., Gruenberg, J., and Zerial, M. (1991) Hypervariable C-terminal domain of rab proteins acts as a targeting signal. *Nature* **353**, 769–772
 37. Steele-Mortimer, O., Clague, M. J., Huber, L. A., Chavrier, P., Gruenberg, J., and Gorvel, J. P. (1994) The N-terminal domain of a rab protein is involved in membrane-membrane recognition and/or fusion. *EMBO J.* **13**, 34–41
 38. Dumas, J. J., Zhu, Z., Connolly, J. L., and Lambright, D. G. (1999) Structural basis of activation and GTP hydrolysis in Rab proteins. *Structure* **7**, 413–423
 39. Brondyk, W. H., McKiernan, C. J., Burstein, E. S., and Macara, I. G. (1993) Mutants of Rab3A analogous to oncogenic Ras mutants. Sensitivity to Rab3A-GTPase activating protein and Rab3A-guanine nucleotide releasing factor. *J. Biol. Chem.* **268**, 9410–9415
 40. Yin, G., Lopes da Fonseca, T., Eisbach, S. E., Anduaga, A. M., Breda, C., Orcellet, M. L., *et al.* (2014) alpha-Synuclein interacts with the switch region of Rab8a in a Ser129 phosphorylation-dependent manner. *Neurobiol. Dis.* **70**, 149–161
 41. Ostermeier, C., and Brunger, A. T. (1999) Structural basis of rab effector specificity: crystal structure of the small G protein Rab3A complexed with the effector domain of rabphilin-3A. *Cell* **96**, 363–374
 42. Bussell, R., Jr., and Eliezer, D. (2001) Residual structure and dynamics in Parkinson's disease-associated mutants of alpha-synuclein. *J. Biol. Chem.* **276**, 45996–46003
 43. Palmer, A. G., 3rd (1993) Dynamic properties of proteins from NMR spectroscopy. *Curr. Opin. Biotechnol.* **4**, 385–391
 44. Bussell, R., Jr., and Eliezer, D. (2003) A structural and functional role for 11-mer repeats in alpha-synuclein and other exchangeable lipid binding proteins. *J. Mol. Biol.* **329**, 763–778
 45. Bussell, R., Jr., and Eliezer, D. (2004) Effects of Parkinson's disease-linked mutations on the structure of lipid-associated alpha-synuclein. *Biochemistry* **43**, 4810–4818
 46. Kishida, S., Shirataki, H., Sasaki, T., Kato, M., Kaibuchi, K., and Takai, Y. (1993) Rab3A GTPase-activating protein-inhibiting activity of Rabphilin-3A, a putative Rab3A target protein. *J. Biol. Chem.* **268**, 22259–22261
 47. Leonard, M., Song, B. D., Ramachandran, R., and Schmid, S. L. (2005) Robust colorimetric assays for dynamin's basal and stimulated GTPase activities. *Methods Enzymol.* **404**, 490–503
 48. Bonini, N. M., and Giasson, B. I. (2005) Snaring the function of alpha-synuclein. *Cell* **123**, 359–361
 49. Dikiy, I., and Eliezer, D. (2012) Folding and misfolding of alpha-synuclein on membranes. *Biochim. Biophys. Acta* **1818**, 1013–1018
 50. Snead, D., and Eliezer, D. (2014) Alpha-synuclein function and dysfunction on cellular membranes. *Exp. Neurobiol.* **23**, 292–313
 51. Sulzer, D., and Edwards, R. H. (2019) The physiological role of alpha-synuclein and its relationship to Parkinson's disease. *J. Neurochem.* **150**, 475–486
 52. Burre, J., Sharma, M., and Sudhof, T. C. (2018) Cell biology and pathophysiology of alpha-synuclein. *Cold Spring Harb. Perspect. Med.* **8**, a024091
 53. Maroteaux, L., Campanelli, J. T., and Scheller, R. H. (1988) Synuclein: A neuron-specific protein localized to the nucleus and presynaptic nerve terminal. *J. Neurosci.* **8**, 2804–2815
 54. Larsen, K. E., Schmitz, Y., Troyer, M. D., Mosharov, E., Dietrich, P., Quazi, A. Z., *et al.* (2006) Alpha-synuclein overexpression in PC12 and chromaffin cells impairs catecholamine release by interfering with a late step in exocytosis. *J. Neurosci.* **26**, 11915–11922
 55. Vargas, K. J., Makani, S., Davis, T., Westphal, C. H., Castillo, P. E., and Chandra, S. S. (2014) Synucleins regulate the kinetics of synaptic vesicle endocytosis. *J. Neurosci.* **34**, 9364–9376
 56. Burre, J., Sharma, M., Tsetsenis, T., Buchman, V., Etherton, M. R., and Sudhof, T. C. (2010) Alpha-synuclein promotes SNARE-complex assembly *in vivo* and *in vitro*. *Science* **329**, 1663–1667
 57. Burre, J., Sharma, M., and Sudhof, T. C. (2014) alpha-Synuclein assembles into higher-order multimers upon membrane binding to promote

- SNARE complex formation. *Proc. Natl. Acad. Sci. U. S. A.* **111**, E4274–4283
58. Sun, J., Wang, L., Bao, H., Premi, S., Das, U., Chapman, E. R., *et al.* (2019) Functional cooperation of alpha-synuclein and VAMP2 in synaptic vesicle recycling. *Proc. Natl. Acad. Sci. U. S. A.* **116**, 11113–11115
 59. Logan, T., Bendor, J., Toupin, C., Thorn, K., and Edwards, R. H. (2017) alpha-Synuclein promotes dilation of the exocytotic fusion pore. *Nat. Neurosci.* **20**, 681–689
 60. Nellikka, R. K., Bhaskar, B. R., Sanghrajka, K., Patil, S. S., and Das, D. (2021) alpha-Synuclein kinetically regulates the nascent fusion pore dynamics. *Proc. Natl. Acad. Sci. U. S. A.* **118**, e2021742118
 61. Hoffmann, C., Sansevrino, R., Morabito, G., Logan, C., Vabulas, R. M., Ulusoy, A., *et al.* (2021) Synapsin condensates recruit alpha-synuclein. *J. Mol. Biol.* **433**, 166961
 62. Breda, C., Nugent, M. L., Estranero, J. G., Kyriacou, C. P., Outeiro, T. F., Steinert, J. R., *et al.* (2015) Rab11 modulates alpha-synuclein-mediated defects in synaptic transmission and behaviour. *Hum. Mol. Genet.* **24**, 1077–1091
 63. Chutna, O., Goncalves, S., Villar-Pique, A., Guerreiro, P., Marijanovic, Z., Mendes, T., *et al.* (2014) The small GTPase Rab11 co-localizes with alpha-synuclein in intracellular inclusions and modulates its aggregation, secretion and toxicity. *Hum. Mol. Genet.* **23**, 6732–6745
 64. Goncalves, S. A., and Outeiro, T. F. (2017) Traffic jams and the complex role of alpha-Synuclein aggregation in Parkinson disease. *Small GTPases* **8**, 78–84
 65. Soper, J. H., Kehm, V., Burd, C. G., Bankaitis, V. A., and Lee, V. M. (2011) Aggregation of alpha-synuclein in *S. cerevisiae* is associated with defects in endosomal trafficking and phospholipid biosynthesis. *J. Mol. Neurosci.* **43**, 391–405
 66. Pfeffer, S. R. (2017) Rab GTPases: master regulators that establish the secretory and endocytic pathways. *Mol. Biol. Cell* **28**, 712–715
 67. Lang, T., and Jahn, R. (2008) Core proteins of the secretory machinery. *Handb. Exp. Pharmacol.* **184**, 107–127
 68. Wang, T. Y., Ma, Z., Wang, C., Liu, C., Yan, D. Y., Deng, Y., *et al.* (2018) Manganese-induced alpha-synuclein overexpression impairs synaptic vesicle fusion by disrupting the Rab3 cycle in primary cultured neurons. *Toxicol. Lett.* **285**, 34–42
 69. Inglis, K. J., Chereau, D., Brigham, E. F., Chiou, S. S., Schobel, S., Frigon, N. L., *et al.* (2009) Polo-like kinase 2 (PLK2) phosphorylates alpha-synuclein at serine 129 in central nervous system. *J. Biol. Chem.* **284**, 2598–2602
 70. Mbefo, M. K., Paleologou, K. E., Boucharaba, A., Oueslati, A., Schell, H., Fournier, M., *et al.* (2010) Phosphorylation of synucleins by members of the Polo-like kinase family. *J. Biol. Chem.* **285**, 2807–2822
 71. Ang, X. L., Seeburg, D. P., Sheng, M., and Harper, J. W. (2008) Regulation of postsynaptic RapGAP SPAR by Polo-like kinase 2 and the SCFbeta-TRCP ubiquitin ligase in hippocampal neurons. *J. Biol. Chem.* **283**, 29424–29432
 72. Seeburg, D. P., and Sheng, M. (2008) Activity-induced Polo-like kinase 2 is required for homeostatic plasticity of hippocampal neurons during epileptiform activity. *J. Neurosci.* **28**, 6583–6591
 73. Seeburg, D. P., Feliu-Mojer, M., Gaiottino, J., Pak, D. T., and Sheng, M. (2008) Critical role of CDK5 and Polo-like kinase 2 in homeostatic synaptic plasticity during elevated activity. *Neuron* **58**, 571–583
 74. George, J. M., Jin, H., Woods, W. S., and Clayton, D. F. (1995) Characterization of a novel protein regulated during the critical period for song learning in the zebra finch. *Neuron* **15**, 361–372
 75. Sevcsik, E., Trexler, A. J., Dunn, J. M., and Rhoades, E. (2011) Allosteric in a disordered protein: Oxidative modifications to alpha-synuclein act distally to regulate membrane binding. *J. Am. Chem. Soc.* **133**, 7152–7158
 76. Follmer, C., Coelho-Cerqueira, E., Yatabe-Franco, D. Y., Araujo, G. D. T., Pinheiro, A. S., Domont, G. B., *et al.* (2015) Oligomerization and membrane-binding properties of covalent adducts formed by the interaction of alpha-synuclein with the toxic dopamine metabolite 3,4-Dihydroxyphenylacetaldehyde (DOPAL). *J. Biol. Chem.* **290**, 27660–27679
 77. Coelho-Cerqueira, E., Carmo-Gonçalves, P., Pinheiro, A., Cortines, J., and Follmer, C. (2013) alpha-Synuclein as an intrinsically disordered monomer – fact or artefact? *FEBS J.* **280**, 4915–4927
 78. Delaglio, F., Grzesiek, S., Vuister, G. W., Zhu, G., Pfeifer, J., and Bax, A. (1995) NMRPipe: a multidimensional spectral processing system based on UNIX pipes [see comments]. *J. Biomol. NMR* **6**, 277–293
 79. Goddard, T., and Kneller, D. (2007) *SPARKY 3.114*, University of California, San Francisco
 80. Eliezer, D. (2012) Distance information for disordered proteins from NMR and ESR measurements using paramagnetic spin labels. *Methods Mol. Biol.* **895**, 127–138